Aeroelastic effects of large blade deflections for wind turbines

Larsen, Torben J.; Hansen, Anders Melchior; Buhl, Thomas

Published in:
Proceedings

Publication date:
2004

Aeroelastic effects of large blade deflections for wind turbines

Torben J. Larsen
Risoe, National Laboratory
P.O. Box 49, 4000 Roskilde, Denmark
torben.juul.larsen@risoe.dk

Anders M. Hansen
Risoe, National Laboratory
P.O. Box 49, 4000 Roskilde, Denmark
anders.melchior.hansen@risoe.dk

Thomas Buhl
Risoe, National Laboratory
P.O. Box 49, 4000 Roskilde, Denmark
thomas.buhl@risoe.dk

Abstract

The objective of the present work is to present the latest results in effects of including large blade deflections in aeroelastic calculations and to quantify the errors of the linearized approach for a modern flexible mega-watt sized turbine.

In this paper three nonlinear approaches have been used to quantify the effects of large deflections. One approach is a rather simple extension of the already existing aeroelastic code HAWC, which changes the calculation basis so that small deflections are assumed around an initially large deflected blade shape. The second approach is based on a multibody formulation of the beam element used in HAWC, where nonlinear effects are included as a result of modelling the blade using several interconnected bodies. The third approach is a co-rotational finite element formulation where each element can be regarded as linear and the nonlinear effects are included by translation and rotation of the local element coordinate system. The results from the three nonlinear approaches are compared with results obtained by the existing HAWC, and the impact on the following main effects (due to large deflections) are addressed:

1. The reduction of the effective radius.
2. The reduction of power production due to the reduced effective radius.
3. The effect of increased torsional inertia of the blade due to the deflected shape.
4. The change of blade frequencies due to changes in inertia and coupling effects.

1 Introduction

Most aeroelastic codes used today are based on modal expansion techniques or finite beam element theory, which for the majority are based on assumptions of small blade deflections and rotations. The validity of these assumptions seems to be less obvious for the new large wind turbines with very soft blade design than it has been previously. Many nonlinearities dealing with large blade deflection exist e.g. regarding material properties, buckling behavior, delamination etc., but these effects are not a part of this analysis. The nonlinearity dealt with in this paper is the effect of calculating the inertia in the deflected location and placing the loads on the deflected structure. Stiffness properties of the blades are still assumed linear.

The turbine chosen in the present investigation is a modern pitch controlled turbine in mega-watt size. The turbine data are modified slightly by assuming shear centers and mass center to be in the center of elasticity of all blade sections. All deflections are normalized with respect to rotor radius, power output is normalized with respect to nominal power and frequencies are normalized with respect to 1P nominal rotational speed.

In section 2 the three methods are described. In section 3 the codes are compared through static calculations and changes in natural frequency as function of deflection are investigated. In the end of this section the effect on power performance and structural loads has been investigated with the modified HAWC approach.

2 Methods

In the following a short description of this code is given together with a explanation of how the new model is implemented.

2.1 The code HAWC

HAWC (Horizontal Axis Wind turbine Code) [1], [2], [3] is an aeroelastic code with the purpose of predicting load response for a horizontal axis two or three bladed wind turbine in time domain. The program is so far considered to represent the state-of-the-art within aeroelastic modelling of wind turbines. The program consists of several sub-packages

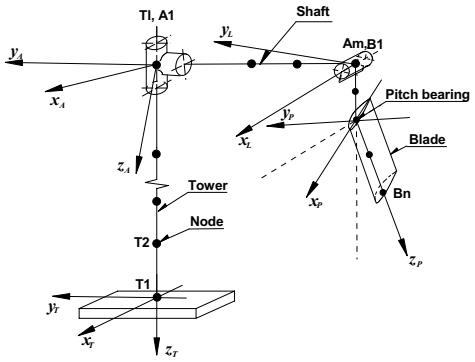

Figure 1: Illustration of the structural model of HAWC.

each dealing with a specific part of the turbine and the surroundings. In the rest of the paper this version of the code is referred to as HAWC_ orig.

The core of the program is the structural model, which is basically a finite element model based on prismatic Timoshenko beam elements. The turbine is divided into three substructures; Tower, nacelle and rotor, see Figure 1. Each substructure has its own coordinate system which, due to a kinematic analysis of the movement and rotation of the substructure, allows for large rotations of the individual substructures with representation of inertia loads inside the substructure. Within a substructure, which consist of several beam elements, the calculation of deflections is linear and all forces are placed on the structure in the un-deformed state, hence large deformations within a substructure are not correctly represented.

Another limitation of the code is that the pitch bearing shown in Figure 1 is not implemented in the same way as the bearing in the tower top and the rotor center. In the tower top and in the rotor center the bearings connect the above mentioned substructures with representation of inertia loads For the pitch bearing this is not a real degree of freedom, hence no inertia loads are included. When the blades are pitched, the node positions are moved to the new position within the substructure coordinate system. This means that the blade position is correct, but the local velocities, accelerations and inertia loads due to the pitch rotation are not included.

Since the loads are placed on the structure in the un-deformed state the pitch moment for a deflected blade is initially incorrect in the HAWC code. The reason for this is that all loads on the blades in a deflected situation will have a moment arm to the pitch axis creating a significant pitch moment

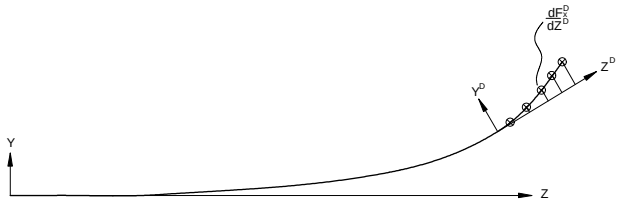

Figure 2: Illustration of pitch moment contributions from blade loads in the deflected location.

contribution, see (1) and Figure 2.

$$\mathbf{M}^D(z) = \int_z^{z_{max}} \mathbf{s}^D(z) \times \frac{d\mathbf{F}^D(z)}{dz} dz \qquad (1)$$

where the index D refers to the local coordinate system in the deformed state illustrated in Figure 2. $\mathbf{s}$ is the deformation vector referring to the local coordinate system in the deflected state D and $\mathbf{F}$ is the external force.

To account for this model limitation a correction procedure has been included, see (2). In the correction procedure an external pitch moment in the blade nodes, which is caused by loads and deflections further out the blade, is applied.

$$\begin{aligned} \mathbf{M}_n &= (\mathbf{s}_{n+1} - \mathbf{s}_n) \times \mathbf{F}_{akk,n+1}, \\ \mathbf{F}_{akk,n} &= \sum_{i=n}^{n_{max}} \mathbf{F}_i \end{aligned} \qquad (2)$$

where $\mathbf{M}$ is a vector $\{M_x, M_y, M_z\}^T$ containing the additional moment contribution from forces further out the blade. $\mathbf{s}$ is the deformation vector referring to the initial substructure coordinate system and $\mathbf{F}_n$ is the external forces in blade number n. Eq. (2) only results in correct pitch moments at the blade root (which is important for dimensioning of pitch systems), but is too large further out the blade. This results in too large pitch rotations at the tip, which increases with the lack of torsional stiffness of the blades.

2.2 Modifications of HAWC

Since the blade deflections for modern wind turbines (especially the pitch controlled turbines) are large compared to what was observed just a few years ago, the errors in the structural linear assumptions mentioned above, should be quantified. A first-hand attempt to include some of the lacking features in HAWC is to move the calculational basis from the un-deformed state to a large deformed state from where small deflections occur. In the rest of this paper this code is referred to as HAWC_ ins.

The original system of equations are formulated

$$\mathbf{M}\ddot{\mathbf{x}} + \mathbf{C}\dot{\mathbf{x}} + \mathbf{K}\mathbf{x} = \mathbf{F} \qquad (3)$$

where $\mathbf{M}$, $\mathbf{C}$, $\mathbf{K}$ and $\mathbf{F}$ are nonlinear matrices constantly updated. If the deformation vector $\mathbf{x}$ is divided into a constant initial vector $\mathbf{x}_i$ and a varying vector $\mathbf{x}_v$ (3) can be rewritten into (4) under the assumption that $\dot{\mathbf{x}}_i \equiv \ddot{\mathbf{x}}_i \equiv 0$

$$\mathbf{M}\ddot{\mathbf{x}}_v + \mathbf{C}\dot{\mathbf{x}}_v + \mathbf{K}\mathbf{x}_v = \mathbf{F} - \mathbf{K}\mathbf{x}_i \tag{4}$$

which is basically the new system of equations to be solved during the time simulation. The matrices $\mathbf{M}$, $\mathbf{C}$ and $\mathbf{K}$ in (4) are in fact not totally identical to the matrices in (3) since the local mass, stiffness and damping properties are transformed from the local element coordinates (where they are unchanged) into substructure coordinates.

The change of basis is carried out at an initial calculation with only the wind speed, pitch angle and rotational speed as input parameters. The static blade deformation is calculated with a special procedure that ensures that the curved length of the blades remain unchanged. The constant loads on the blades are stored in a vector, which is later used to subtract the loads during time simulation so only relative loads are used to calculate deformations from the initially deflected basis. In the bearing node between shaft and rotor the subtracted forces are added to the shaft to ensure that loads on the shaft and tower are absolute and not relative.

Since the time simulation only includes relative forces and deflections on the rotor, the initial reaction forces and deflections are added to the relative forces and deflections in the write out of load and deflection sensors.

2.3 Multi-body formulation

The multi-body approach has several similarities with the existing formulation of the current HAWC, but is formulated in a much more general way. As for the HAWC code the wind turbine is divided into several substructures, also referred to as bodies. This is done by using the multi-body formulation to describe the behavior of each substructure (cf. [4]). The substructures includes its own coordinate system with calculation of internal inertia loads when this coordinate system is moved in space, hence large rotations and translation of the substructure is accounted for. Inside a substructure the formulation is linear, which means that e.g. large deflection effects of the blades are taken into consideration when the blade is subdivided into several substructures. The essential difference for the multi-body formulation to e.g. the current HAWC is the formulation of differential equations (mass, stiffness and damping matrices), where the different substructures mass, stiffness and damping elements are isolated from the rest of the equations, hence it is very easy to change from one type of substructure to another. The coupling between the substructures is done through introduction of coupling constraints in the equations, e.g. bearing properties are formulated as a special constraint.

The amount of substructures is optional and so is the location, however, choosing to few bodies will result in a reduction of a nonlinear problem to a linear.

2.4 Co-rotational formulation

Taking into account large displacements and rotations requires a geometrical non-linear finite element formulation. An alternative to the multi-body formulation is the co-rotational approach. The essential idea is to split the overall response into a rigid body rotation and translation, and the deformation of the element. This is achieved by assigning a local coordinate system to each element which rotates and translate with the element. If an element is chosen to have a proper length the deformations are small relative to the local coordinate system and a linear representation of the element can be used. The geometrical non-linear effects are included in the translation and rotation of the local coordinate system.

In the following the methodology in [5], [6] and [7] is used. Only few equations are shown here. For a full detailed description please see [5] and references therein.

As mentioned, the deformations and rotations can be regarded as small and linear in the local frame coordinate system. This leads to the following simple relation between the local nodal forces and local nodal displacements.

$$\mathbf{f}_l = \mathbf{K}_l \mathbf{q}_l \tag{5}$$

The term $\mathbf{K}_l$ if the usual linear stiffness matrix for the element used.

The nodal triads are defined as vectors for each direction denoted $\mathbf{t}_1$, $\mathbf{t}_2$ and $\mathbf{t}_3$ for nodal point one and $\mathbf{q}_1$, $\mathbf{q}_2$ and $\mathbf{q}_3$ for nodal point two. The nodal triads are assembled in matrices denoted $\mathbf{T}$ and $\mathbf{Q}$ where each row in the matrices are the previous mentioned vectors. The triad for the local frame for the beam element is equivalent a matrix assembled by the vectors for the three directions.

The global variables can be found from the local variables by a transformation matrix as follows

$$\partial \mathbf{q}_l = \mathbf{F} \partial \mathbf{q} \tag{6}$$

Thus giving the global internal forces as

$$\mathbf{f} = \mathbf{F}^T \mathbf{f}_l = \mathbf{F}^T \mathbf{K}_l \mathbf{q}_l \tag{7}$$

The transformation matrix $\mathbf{F}$ is a 12 by 12 matrix. Each row is a vector denoted $\mathbf{f}_1$, $\mathbf{f}_2$, ..., $\mathbf{f}_{12}$ and can be derived from the element node triads, the element base triad and some rotation matrices given in [5].

The equilibrium can be written as

$$\partial \mathbf{q}_i = (\mathbf{K}_{t1} + \mathbf{K}_{t\sigma})\partial \mathbf{p} \tag{8}$$

where $\mathbf{K}_{t1}$ is the linear stiffness matrix transformed from the local coordinate systems to the global coordinate system ($\mathbf{K}_{t1} = \mathbf{F}^T \mathbf{K}_l \mathbf{F}$). The term $\mathbf{K}_{t\sigma}$ is geometric stiffness matrix. The details in the derivations of the term the authors suggest to read reference [5] and references therein.

The dynamic equations are derived on the basis of the Newmark method. The extension of this method compared to standard Newmark is to include the dynamic equilibrium with rotations. For further detail please read chapter 24 in [5].

3 Simulations

The three different approaches have been compared in different situations. The first calculation is a simple calculation at standstill with deterministic static loads on the blades. Blade deflection shapes are compared. Then the dynamics have been compared by exciting the turbine vibration modes at standstill to investigate the frequency change as function of deflection.

Since only HAWC and the modified HAWC approach has included aerodynamic loading at present time, only this and the original HAWC formulation has been used to investigate the influence of large deflections on loads and power production.

3.1 Static blade deflection

To compare the codes in a simple way, a static deterministic load in the blade flap direction linearly increasing from the hub to the tip is applied. Loads and deflection are compared in Figure 3 and 4. The load size shown in Figure 3 and 4 is the integrated flapwise loading of one blade. For the two HAWC version the flapwise loads are placed on the structure in the blade root coordinate system. For the multi-body and the co-rotational approaches the forces moves according to the deflection, which is the reason for the differences in edgewise blade root moments. The flap and edgewise deflection is almost identical, but for the torsional rotation of the tip, differences are seen. The HAWC calculations show a rotation of 5.7° when the blades are deflected 0.27 rotor radius. The explanation for this is the torsion moment correction procedure shown in eq. (2) which results in too high torsional moments at the outer part of the blades where the torsional stiffness is low. The multi-body shows a limited torsional rotation of 0.5°, whereas the co-rotational formulation shows a rotation of 0.2°.

What is also important to notice is the reduced flapwise deflection of the nonlinear approaches compared to the original linear HAWC approach (see Figure 4). This difference in deflection could very well be of importance for blade designers.

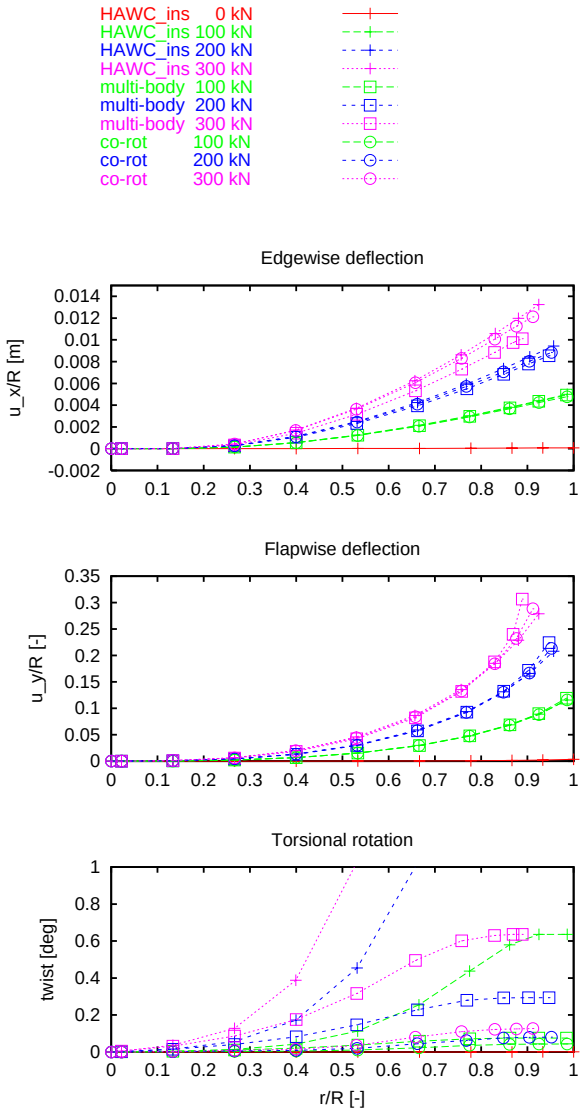

Figure 3: Calculated blade deflection shapes.

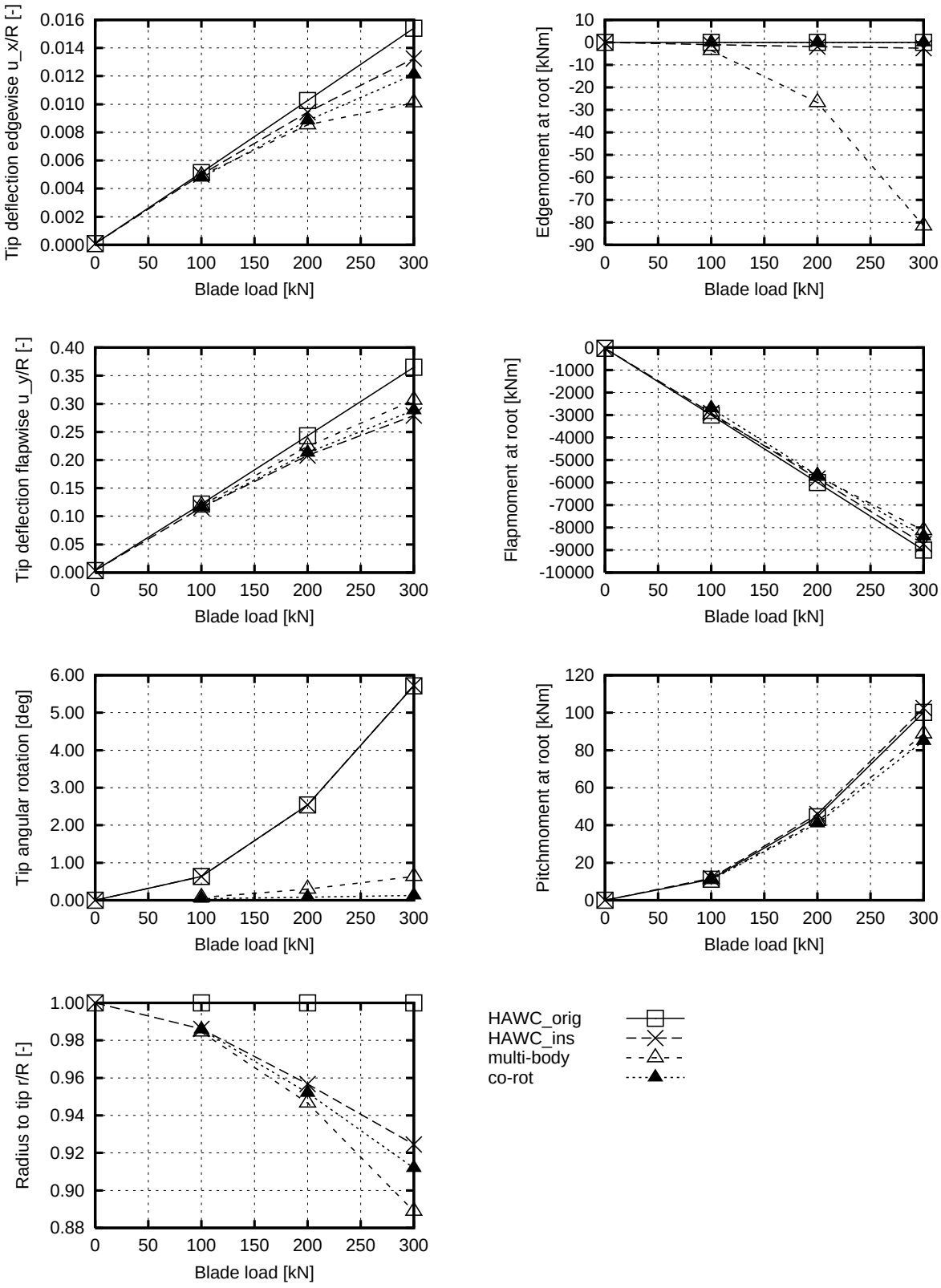

Figure 4: Load and deflections for the static load cases.

Rotor mode	Frequency [-]
1^{st} tower	2.32
1^{st} yaw	3.97
1^{st} tilt	4.16
1^{st} symmetric flap	4.49
1^{st} shaft torsion	5.06
1^{st} edge 1	5.47
1^{st} edge 2	5.62

Table 1: Frequencies at standstill normalized with 1P rotation frequency.

3.2 Dynamic analysis

As the blades are deflected their inertia and stiffness with respect to the blade root coordinate system changes, hence the natural frequencies changes as function of deflection. This is most obviously understood dealing with the inertia around the pitch axis. For a blade deflected in the flapwise direction, the inertia around the pitch axis increases significantly. If the blade torsional frequency was mainly determined by the inertia around the pitch axis and the stiffness in the pitch actuator, this frequency would decrease when the blade is deflected. However since the stiffness of the pitch actuator system is not included in the models in this paper, the torsional frequency is merely determined by the inertia around the local bending centers and the torsional stiffness of the blade sections, which is the reason that the torsional frequency in the calculations remain unchanged (not shown).

To investigate the change in frequencies, due to the deflection, a simulation is carried out where the turbine at standstill is excited with a white noise random force in the tower top. Hereby all rotor natural frequencies are excited. The frequency shift is observed with power spectral analysis of the blade root flap, edge and pitch moments at the different load levels as shown in Figure 5, 6 and 7. In the original HAWC no change in frequency occurs, whereas an increment in blade flap and edgewise frequency is seen in HAWC_ INS. In the multi-body formulated code an increase in flap frequency is seen, but the edgewise frequency remain more or less unchanged. The reason for the increased natural frequency of the blade flap frequency is the changed inertia of the rotor. As the blade deflects, the absolute distance of all blade inertia to the blade root, is reduced, leading to higher flap frequency. For the blade edgewise frequency the case is more complex. As the blade is deflected flapwise the mode shape of the edgewise frequency couples to the torsional stiffness of the blade, which have a stiffness reducing effect. At the same time a stiffness increasing effect occurs since the external loads on the blade creates a torsional moment that twist the blades, which mean that the external loads in the deflected case has an increasing stiffness effect. The two effects counteract each other leaving the frequency more or less unchanged. The reason that the HAWC_ INS model predicts the edgewise frequency too high, compared to the multi-body code, is due to the conservative expression in eq. (2) which overpredicts the torsional moment locally on the blade, hence the stiffness increasing effect is too high.

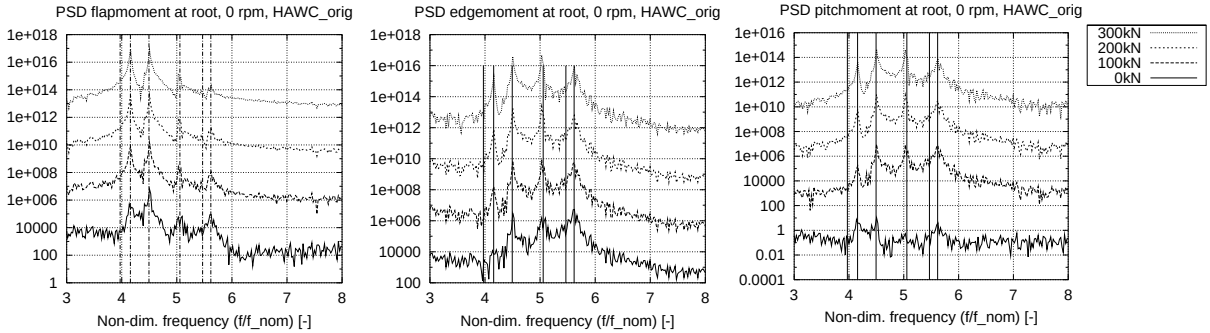

Figure 5: PSD at standstill. HAWC_ orig. Frequencies remains unchanged.

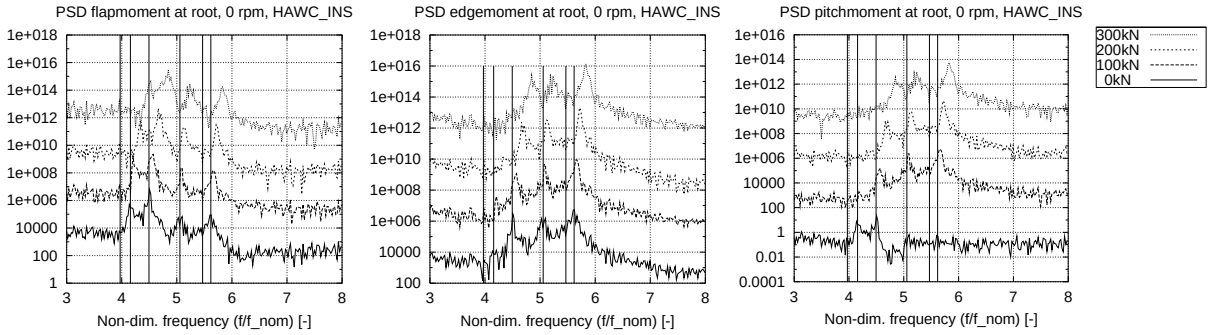

Figure 6: PSD at standstill. HAWC_ INS. The blade flap and edgewise frequencies are increasing due to the blade deflection.

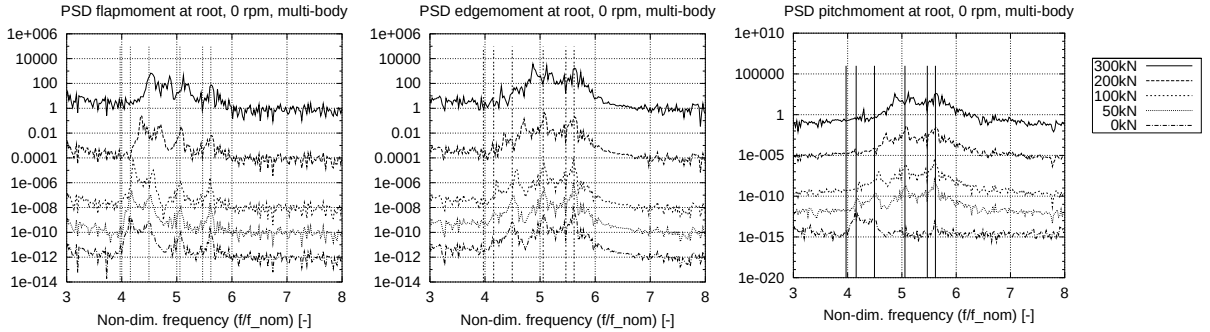

Figure 7: PSD at standstill. Multi-body. The blade flap frequency is increasing due to the blade deflection, but the edgewise frequency remain unchanged.

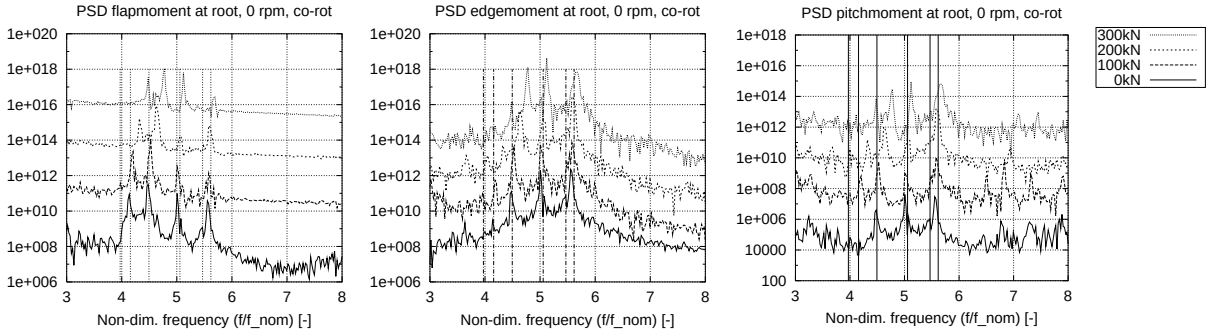

Figure 8: PSD at standstill. Co-rotational formulation. The blade flap frequency is increasing due to the blade deflection and the edgewise frequency increases slightly.

Wind speed	Power production		Dev. area
	HAWC_orig	HAWC_INS	HAWC_INS
4	1.000	0.994	0.9996
6	1.000	0.986	0.9983
8	1.000	0.975	0.9949
10	1.000	0.975	0.9905
12	1.000	0.979	0.9870
14	1.000	1.000	0.9832

Table 2: Power production at different wind speeds - normalized with respect to HAWC_ orig calculations. In the last column is shown the effective rotor area in the HAWC_ ins normalized with respect to the original area.

3.3 Power performance

As the blades deflects, the effective rotor radius changes, which leads to a change in power performance. To investigate the influence on the chosen pitch regulated turbine a series of power curves have been performed. Power performance is calculated for a turbine with stiff and soft blades. The rotor has no cone angle. The results can be seen in Table 2. The basic aerodynamic calculation method is a BEM-method with tip-loss correction according to Prandtl, see [8].

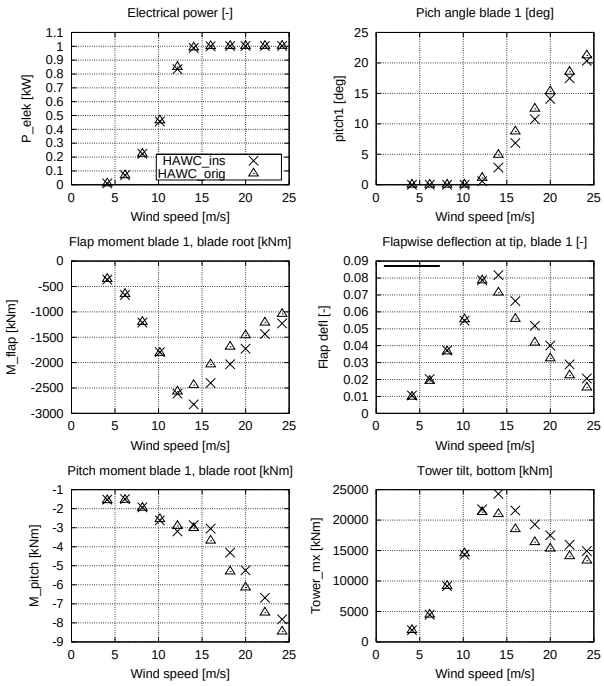

Figure 9: Mean levels of selected sensors of load simulations.

3.4 Loads and deflections

To compare the influence on loads a fatigue load spectrum based on IEC61400-1 class 1B has been calculated. The load cases are normal production cases with winds speed ranging from 4 m/s to 24 m/s. From Figure 9 is seen that the influence on large deflections results in lower power production at low wind speed and a lower pitch angle setting at high wind speed, which is a direct result of the lower effective rotor radius. This can also be seen in the tower bottom tilt moment. The mean flap moment increases at high wind speed, mainly due to the change in pitch setting. The pitch moment seem to decrease in average. From the simulations no main tendency in change of fatigue load levels could be obtained.

4 Conclusion

The influence of including the effect of large deflections in wind turbine load simulations has been investigated. In the investigation a modification of the aeroelastic code HAWC has been carried out so that small deflections are assumed around an initially large deflected blade shape. A second method used in the investigation is a multi-body formulated structural code, which has the nonlinear effect included as a result of dividing the blade into several inter-connected bodies. The third method is the co-rotational formulation where each element includes its own coordinate system.

The primary effect of including the influence on large deflections is that the effective rotor area changes. This change in effective radius causes a reduction in power output at low wind speeds and a change in pitch angle setting at high wind speeds. At high wind speed this change in pitch angle setting leads to a higher flapwise mean load level. The mean level of the rotor thrust is reduced due to the reduced rotor area. No main differences regarding fatigue load levels could be obtained from the load simulations.

For the structural behaviour of the blades an increment in flap frequency is seen as function of deflection, which is mainly caused by a change in inertia as the blade deflects. The edgewise frequency seems to remain constant due to two counteracting stiffness effects. As the blade is deflected in the flapwise direction the inertia of the edgewise mode-shape couples to the torsional stiffness of the blade creating a decrease in frequency which is counteracted by the coupling between the external loads coupling to torsion of the blade in the deflected shape.

The effects of large deflection are for the modern turbine in a size where it is no longer totally neglectable. Fortunately the main effect is regarding power production, which does not results in safety issues. The linear codes are conservative regard-

ing tip deflections, but regarding fatigue loads there seems to be only minor significant differences. As the size of the turbines increases the effects will most likely increase as well.

References

[1] J. T. Petersen. The Aeroelastic Code HawC - Model and Comparisons. In *28th IEA Experts Meeting: 'State of the Art of Aeroelastic Codes'*. DTU, Lyngby, 1996.

[2] J. T. Petersen. *Kinematically Nonlinear Finite Element Model of a Horizontal Axis Wind Turbine. Part 1: Mathematical Model and Results*. PhD thesis, Risoe, National Laboratory, 1990.

[3] J. T. Petersen. *Kinematically Nonlinear Finite Element Model of a Horizontal Axis Wind Turbine. Part 2: Supplement. Inertia Matrices and Aerodynamic Model*. PhD thesis, Risoe, National Laboratory, 1990.

[4] A. A. Shabana. *Dynamics of Multibody Systems*. Cambridge University Press, University of Illinois at Chicago, 2nd edition, 1998.

[5] M.A. Crisfield. *Non-linear Finite Element Analysis of Solids and Structures*, volume 2 Advanced topics. John Wiley and Sons, 1997.

[6] M.A. Crisfield. A consistent co-rotational formulation for non-linear, three-dimensional, beam-elements. *Comp. Meth. Appl. Mech. Eng.*, 81:131–150, 1990.

[7] M.A. Crisfield, U. Galvanetto, and G. Jelenić. Dynamics of 3-d co-rotational beams. *Computational Mechanics*, 20:507–519, 1997.

[8] H. Glauert. *Aerodynamic theory: A general review of progress*, volume IV, pages 169–360. Peter Schmidt Publisher, Inc., 1976.